Weak-light superluminal vector solitons in a room-temperature four-level active-Raman-gain medium

Chao Hang[1] and Guoxiang Huang[1,2,*]

[1]*State Key Laboratory of Precision Spectroscopy, and Department of Physics, East China Normal University, Shanghai 200062, China*
[2]*Department of Physics, Zhejiang Normal University, Jinhua 321004, Zhejiang, China*
**Corresponding author: gxhuang@phy.ecnu.edu.cn*

Received October 9, 2008; revised November 17, 2008; accepted December 17, 2008; posted December 23, 2008 (Doc. ID 102452); published February 6, 2009

We propose a scheme to generate vector optical solitons in a four-level active-Raman-gain medium. We show that this scheme, which is fundamentally different from that using optical fibers and that via electromagnetically induced transparency, is capable of achieving robust vector optical solitons with superluminal propagating velocity. We demonstrate that such vector optical solitons can be generated at room temperature and with very low light intensity. We investigate also the interaction between two superluminal vector optical solitons and point out that their elastic and inelastic colliding properties can be used to design rapidly responding optical soliton switching and logic gates. © 2009 Optical Society of America

OCIS codes: 270.0270, 190.3270.

1. INTRODUCTION

Most vector optical solitons are solutions of two coupled nonlinear Schrödinger (NLS) equations, which describe the envelope evolution of two polarization components of an electromagnetic field in a nonlinear optical medium. There has been much interest focused on the temporal [1–6] and spatial [7–9] vector optical solitons in various physical systems, which is due to their promising applications for optical information processing and transmission [10,11].

As far as we know, up to now vector optical solitons are produced in passive media such as optical fibers, waveguides, and photorefractive materials [1–11] (except for the work by Cundiff *et al.* where vector optical solitons are generated in a pumped fiber laser [12]), in which far-off resonance excitation schemes are employed in order to avoid unmanageable optical attenuation and distortion. As a result, nonlinear effect in these media is very weak and, hence, to form a vector optical soliton very high input light power is needed. Furthermore, because of the lack of distinctive energy levels and selection rules, an active control of vector optical solitons in such far-off resonant systems is difficult to sustain. In addition, vector optical solitons produced in far-off resonant media generally travel with a speed very close to c, the speed of light in vacuum, and they require an extended propagation distance in order to generate.

In recent years, considerable attention has been paid to the study of optical propagation via electromagnetically induced transparency (EIT), in which an on-resonance excitation scheme is used [13]. Based on several interesting features under weakly driven EIT conditions, the possibility of generating ultraslow optical solitons has been explored recently [14–18]. However, weakly driven EIT schemes still have some inherent drawbacks, including the significant signal field attenuation and distortion at room temperature and the very long response time due to the ultraslow propagating velocity. These drawbacks may become obstacles in developing further applications of room-temperature and ultrafast all-optical devices for EIT schemes.

The study on superluminal propagation of light (i.e., light propagates in a medium with apparent group velocity exceeding c, or even becoming negative) is a topic with a very long history [19]. Chu and Wong [20] presented the first experimental demonstration of superluminal propagation of an optical wavepacket in an absorptive medium. In order to avoid substantial attenuation and to obtain a stable superluminal propagation, Chiao [21,22] *et al.* suggested the use of an on-resonant, active Raman gain (ARG) medium with an inverted atomic population. Later on, there appeared a large amount of theoretical and experimental investigations of superluminal propagation in ARG atomic media [23–29]. An ARG system is fundamentally different from that based on EIT. The signal field in the ARG system operates in a stimulated Raman emission mode and, hence, may propagate with group velocity faster than c, and it has no attenuation or distortion even when the system works at room temperature.

Recently, it has been shown that a gain-assisted, large and rapidly responding Kerr effect is possible by using a room-temperature ARG medium [30]. A fast-responding nonlinear phase shifter using an ARG system has also been demonstrated [31]. These important works hint at the possibility of realizing superluminal optical solitons in ARG media. The authors of [32,33] made interesting theoretical studies on superluminal solitons in resonant atomic media. However, in those works a short-pulse con-

dition was used to neglect decay rates of atomic levels, i.e., the solutions require the system to work in a coherent transient regime. Without using such short-pulse condition, recent studies [34,35] have shown that superluminal optical solitons can be generated and propagate stably in a three-level ARG medium when working outside of a coherent transient regime.

In this paper, a four-level tripod system, which can be realized by ^{87}Rb atoms, with an ARG configuration is proposed to generate superluminal vector optical solitons. Such a scheme is fundamentally different from those using passive media [1–12] and those via EIT-based atomic media [18]. The vector optical solitons predicted here have superluminal propagating velocity and can be produced at room temperature and under very low light intensity. The interaction between superluminal vector optical solitons display interesting elastic and inelastic colliding properties, which may have potential applications in designing rapidly responding, low-light-level soliton switching and logic gates.

The remainder of the paper is arranged as follows. In Section 2, the theoretical model under study is introduced, and its solution in a linear regime is presented. In Section 3, an asymptotic expansion on Maxwell–Schrödinger equations is made, and coupled NLS equations governing the time evolution of two polarization components of a signal field are derived by means of a method of multiple scales. In Section 4, weak-light superluminal vector optical soliton solutions are provided, and their stability is discussed by means of numerical simulations. In the same section, a numerical study is carried out to explore the collision property of the superluminal vector optical solitons. Finally, the last section contains a discussion and summary of the main results of our work.

2. MODEL AND SOLUTIONS IN THE LINEAR REGION

We consider a four-level, tripod atomic system interacting with a weak, linear-polarized pulsed signal field of central frequency $\omega_s/2\pi$ and a strong, linear-polarized continuous wave pump field of frequency $\omega_P/2\pi$, respectively. The two circular-polarized components of the signal field drive, respectively, the transitions from $|2\rangle\leftrightarrow|4\rangle$ and $|3\rangle\leftrightarrow|4\rangle$, while the pump field drives the transitions from $|1\rangle\leftrightarrow|4\rangle$ (see Fig. 1), respectively. Here, states $|1\rangle, |2\rangle$, and $|3\rangle$ are sublevels of one atomic state due to a Zeeman split induced by an applied magnetic field B.

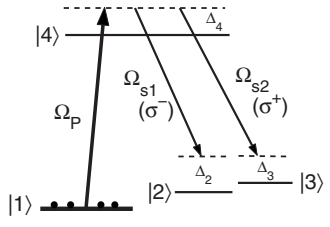

Fig. 1. Energy-level diagram and excitation scheme of a four-state tripod atomic system interacting with a strong, linear-polarized continuous-wave pump field of Rabi frequency Ω_P and a weak, pulsed signal field of two circular-polarized components σ^+ and σ^- with Rabi frequencies Ω_{s1} and Ω_{s2}, respectively. Δ_j is the detuning between the corresponding optical field and the level $|j\rangle$.

The electric field of the system can be written as $\mathbf{E}=(\hat{\varepsilon}_+\mathcal{E}_{s+}+\hat{\varepsilon}_-\mathcal{E}_{s-})\exp[i(k_sz-\omega_st)]+\hat{\mathbf{e}}_P\mathcal{E}_P\exp[i(\mathbf{k}_P\cdot\mathbf{r}-\omega_Pt)]+$c.c.. Here $\hat{\varepsilon}_+=(\hat{\mathbf{x}}+i\hat{\mathbf{y}})/\sqrt{2}$ ($\hat{\varepsilon}_-=(\hat{\mathbf{x}}-i\hat{\mathbf{y}})/\sqrt{2}$) is the signal field unit vector of the σ^+ (σ^-) circular polarization component with the envelope $\mathcal{E}_{s+}$ ($\mathcal{E}_{s-}$), which drives the transition $|3\rangle\leftrightarrow|4\rangle$ ($|2\rangle\leftrightarrow|4\rangle$). $\hat{\mathbf{e}}_P$ is the unit vector of the pump field with the envelope $\mathcal{E}_P$. For simplicity, we have chosen the wavevector direction of the signal field along the z axis.

The Hamiltonian of the system is $\hat{H}=\hat{H}_0+\hat{H}'$, where $\hat{H}_0$ describes a free atom and $\hat{H}'$ describes the interaction between the atom and the optical field. In the Schrödinger picture, the state vector of the system is expressed by $|\Psi(t)\rangle_s=\Sigma_{j=1}^4C_j(z,t)|j\rangle$, where $|j\rangle$ is the eigenstate of $\hat{H}_0$. Under electric-dipole and rotating-wave approximations, the Hamiltonian of the system takes the form

$$\hat{H}=\sum_{j=1}^{4}\varepsilon_j|j\rangle\langle j|+\hbar\{\Omega_P\exp[i(\mathbf{k}_P\cdot\mathbf{r}-\omega_Pt)]|4\rangle\langle 1|+\Omega_{s1}\times\exp[i(k_sz-\omega_st)]|4\rangle\langle 2|+\Omega_{s2}\times\exp[i(k_sz-\omega_st)]|4\rangle\langle 3|+\text{H.c.}\},\quad(1)$$

where ε_j is the energy of state $|j\rangle$, $\Omega_{s1}=(\mathbf{p}_{42}\cdot\hat{\varepsilon}_-)\mathcal{E}_{p-}/\hbar$, $\Omega_{s2}=(\mathbf{p}_{43}\cdot\hat{\varepsilon}_+)\mathcal{E}_{p+}/\hbar$, and $\Omega_P=(\mathbf{p}_{41}\cdot\hat{\mathbf{e}}_P)\mathcal{E}_c/\hbar$ are relevant half Rabi frequencies, with $\mathbf{p}_{ij}$ being the electric dipole matrix element associated with the transition from $|j\rangle$ to $|i\rangle$.

For convenience, we employ an interaction picture to eliminate fast spatial-temporal variables, which can be obtained by making the transformation $C_j=A_j\exp\{i[\mathbf{k}_j\cdot\mathbf{r}-(\varepsilon_j/\hbar+\Delta_j)t]\}$, with $\mathbf{k}_1=0$, $\mathbf{k}_2=\mathbf{k}_3=k_P\mathbf{e}_P-k_s\mathbf{e}_z$, and $\mathbf{k}_4=k_P\mathbf{e}_P$. The detunings Δ_j are defined as $\Delta_2=\omega_P-\omega_s-(\varepsilon_2-\varepsilon_1)/\hbar$, $\Delta_3=\omega_P-\omega_s-(\varepsilon_3-\varepsilon_1)/\hbar$, and $\Delta_4=\omega_P-(\varepsilon_4-\varepsilon_1)/\hbar$. It is noteworthy that$\Delta\equiv(\varepsilon_3-\varepsilon_2)/\hbar=(2\mu_B/\hbar)gB$ is the Zeeman shift of atomic sublevels with μ_B, the Bohr magneton, and g, the gyromagnetic factor. Then we obtain the Hamiltonian in the interaction picture

$$\hat{H}_{\text{int}}=\hbar[\Delta_2|2\rangle\langle 2|+\Delta_3|3\rangle\langle 3|+\Delta_4|4\rangle\langle 4|]-\hbar[\Omega_P|4\rangle\langle 1|+\Omega_{s1}|4\rangle\times\langle 2|+\Omega_{s2}|4\rangle\langle 3|+\text{H.c.}].\quad(2)$$

Using the Schrödinger equation $i\hbar\partial|\Psi(t)\rangle_{\text{int}}/\partial t=H_{\text{int}}|\Psi(t)\rangle_{\text{int}}$ with $|\Psi(t)\rangle_{\text{int}}=(A_1,A_2,A_3,A_4)^T$ (T represents transpose) one can readily obtain the equations governing atomic response

$$\left(i\frac{\partial}{\partial t}+d_{2,3}\right)A_{2,3}+\Omega_{s1,s2}^*A_4=0,\quad(3a)$$

$$\left(i\frac{\partial}{\partial t}+d_4\right)A_4+\Omega_PA_1+\Omega_{s1}A_2+\Omega_{s2}A_3=0,\quad(3b)$$

with $\Sigma_{j=1}^4|A_j|^2=1$, where A_j ($j=1$ to 4) is the probability amplitude of the bare atomic state $|j\rangle$. Note that in Eq. (3) we have defined $d_j=\Delta_j+i\gamma_j$ ($j=2,3,4$), with γ_j being the decay rate of the level $|j\rangle$. We assume that the system works at room temperature, and thus the Doppler effect is significant. In order to suppress a large gain and the Doppler effect, we choose the one-photon detuning Δ_4 to be much larger than any Rabi frequencies, Doppler broadened line

widths, atomic decay rates, and frequency shift induced by the pump field.

To obtain the equations of motion for $\Omega_{s1}(z,t)$ and $\Omega_{s2}(z,t)$, we use the Maxwell equation

$$\nabla^2\mathbf{E} - \frac{1}{c^2}\frac{\partial^2\mathbf{E}}{\partial t^2} = \frac{1}{\varepsilon_0 c^2}\frac{\partial^2\mathbf{P}}{\partial t^2} \tag{4}$$

with

$$\mathbf{P} = \mathcal{N}_a\{\mathbf{p}_{41}A_4A_1^* \exp[i(\mathbf{k}_P\cdot\mathbf{r} - \omega_P t)] + \mathbf{p}_{42}A_4A_2^* \exp[i(k_s z - \omega_s t)] + \mathbf{p}_{43}A_4A_3^* \exp[i(k_s z - \omega_s t)] + \text{c.c.}\}.$$

Under a slowly varying envelope approximation, Eq. (4) is reduced to

$$i\left(\frac{\partial}{\partial z} + \frac{1}{c}\frac{\partial}{\partial t}\right)\Omega_{s1,s2} + \kappa A_4 A_{2,3}^* = 0, \tag{5}$$

where $\kappa = \mathcal{N}_a\omega_s|\mathbf{p}_{24}|^2/(2\varepsilon_0 c\hbar) \simeq \mathcal{N}_a\omega_s|\mathbf{p}_{34}|^2/(2\varepsilon_0 c\hbar)$ with $\mathcal{N}_a$ being the atomic density, $\mathbf{p}_{24}$ ($\mathbf{p}_{34}$) the electric-dipole matrix element for the transition from $|2\rangle$ ($|3\rangle$) to $|4\rangle$.

Before solving the coupled nonlinear Eqs. (3) and (5), a simple physical analysis on linear property of the system is useful. We assume that atoms are initially populated in the state $|1\rangle$. Equations (3) and (5) admit the steady-state solution $A_1 = 1/\sqrt{1+|\Omega_P/d_4|^2}$, $A_2 = A_3 = 0$, $A_4 = -\Omega_P/(d_4\sqrt{1+|\Omega_P/d_4|^2})$, and $\Omega_{s1} = \Omega_{s2} = 0$. It is easy to obtain the solution of linear excitation around this steady state, which is proportional to $\exp\{i[K(\omega)z - \omega t]\}$. The dispersion relation of the linear excitation displays two branches, which are given by

$$K_{1,2} = \frac{\omega}{c} + \frac{\kappa|\Omega_P|^2}{(\omega - d_{2,3}^*)(|d_4|^2 + |\Omega_P|^2)}, \tag{6}$$

corresponding to σ^- and σ^+ components of the signal field, respectively.

By Taylor-expanding Eq. (6) around the central frequency of the signal field ω_s (i.e., at $\omega = 0$) we obtain $K_1(\omega) = K_{01} + K_{11}\omega + K_{21}\omega/2 + \mathcal{O}(\omega^3)$ and $K_2(\omega) = K_{02} + K_{12}\omega + K_{22}\omega/2 + \mathcal{O}(\omega^3)$, with $|K_{ij} = (\partial^j K_j(\omega)/\partial\omega^i)|_{\omega=0}$. Here, $K_{01} = \varphi_1 + i\alpha_1/2$ ($K_{02} = \varphi_2 + i\alpha_2/2$) with $\varphi_1 = -\kappa|\Omega_P|^2\Delta_2/(|d_2|^2|d_4|^2)$ ($\varphi_2 = -\kappa|\Omega_P|^2\Delta_3/(|d_3|^2|d_4|^2)$) and $\alpha_1 = -2\kappa|\Omega_P|^2\gamma_2/(|d_2|^2|d_4|^2)$ ($\alpha_2 = -2\kappa|\Omega_P|^2\gamma_3/(|d_3|^2|d_4|^2)$) being the phase shift and absorption coefficient, respectively. Note that the two polarization components of the signal field in fact acquire gain during propagation because α_1 and α_2 are always negative. This is very different from an EIT-based system, which is inherently absorptive. The group velocity of the σ^- (σ^+) component of the signal field is given by $V_{g1} = 1/\mathrm{Re}(K_{11}) = c/n_{g1}$ ($V_{g2} = 1/\mathrm{Re}(K_{12}) = c/n_{g2}$) with the group index $n_{g1} = 1 + c\kappa|\Omega_P|^2(\gamma_2^2 - \Delta_2^2)/(|d_2|^4|d_4|^2)$ ($n_{g2} = 1 + c\kappa|\Omega_P|^2(\gamma_3^2 - \Delta_3^2)/(|d_3|^4|d_4|^2)$). Thus, if $\gamma_2 > \Delta_2$ ($\gamma_3 > \Delta_3$) one obtains $0 < V_{g1} < c$ ($0 < V_{g2} < c$) (corresponding to a subluminal propagation); if $\gamma_2 < \Delta_2$ ($\gamma_3 < \Delta_3$) one has $V_{g1} > c$ ($V_{g2} > c$) or $V_{g1} < 0$ ($V_{g2} < 0$) (corresponding to a superluminal propagation). K_{21} (K_{22}) represents the group-velocity dispersion of the σ^- (σ^+) component of the signal field.

3. ASYMPTOTIC EXPANSION AND NONLINEAR ENVELOPE EQUATIONS

We know that group-velocity dispersion will result in a spreading of the signal field, which is harmful for optical information processing. It is natural to use nonlinear effects, i.e., self-phase modulation (SPM) and cross-phase modulation (CPM) of the signal field, to balance dispersion-induced spreading. To investigate the influence of both nonlinear and dispersion effects in a transparent way, we apply a method of multiple scales to derive nonlinear envelope equations of the signal field. For this aim we make the asymptotic expansion $A_j = \sum_{l=0}^{\infty}\varepsilon^l A_j^{(l)}$ ($j = 1$ to 4), $\Omega_{s1} = \sum_{l=1}^{\infty}\varepsilon^l\Omega_{s1}^{(l)}$, and $\Omega_{s2} = \sum_{l=1}^{\infty}\varepsilon^l\Omega_{s2}^{(l)}$ with $A_1^{(0)} = 1/\sqrt{1+|\Omega_P/d_4|^2}$, $A_2^{(0)} = A_3^{(0)} = 0$, and $A_4^{(0)} = -\Omega_P/(d_4\sqrt{1+|\Omega_P/d_4|^2})$, where ε is a small parameter characterizing the amplitude of the signal field. To obtain a divergence-free expansion, all quantities on the right-hand side of the expansion are considered as functions of the multiscale variables $z_l = \varepsilon^l z$ ($l = 0$ to 2) and $t_l = \varepsilon^l t$ ($l = 0$, 1). Substituting such expansion into Eqs. (3)–(5), we obtain a series of equations for $A_j^{(l)}$, $\Omega_{s1}^{(l)}$, and $\Omega_{s2}^{(l)}$ ($j = 1,2,3,4$; $l = 1,2,3,\ldots$).

The leading (i.e., $O(\varepsilon)$) order solution is given by $\Omega_{s1}^{(1)} = F_1\exp(i\theta_1)$ ($\Omega_{s2}^{(1)} = F_2\exp(i\theta_2)$) with $\theta_1 = K_1(\omega)z_0 - \omega t_0$ ($\theta_2 = K_2(\omega)z_0 - \omega t_0$), here F_1 (F_2) is a yet to be determined envelope function of the σ_- (σ_+) component depending on the slow variables t_1 and z_j ($j = 1,2$). We also obtain $A_1^{(1)} = A_4^{(1)} = 0$ and $A_2^{(1)} = [(K_1^* - \omega/c)F_1^*/(\kappa A_4^{*(0)})]\exp(-i\theta_1^*)$ ($A_3^{(1)} = [(K_2^* - \omega/c)F_2^*/(\kappa A_4^{*(0)})]\exp(-i\theta_2^*)$).

At the second ($O(\varepsilon^2)$) order, divergence-free conditions for the second-order solution require

$$i[\partial F_1/\partial z_1 + (1/V_{g1})\partial F_1/\partial t_1] = 0, \tag{7a}$$

$$i[\partial F_2/\partial z_1 + (1/V_{g2})\partial F_2/\partial t_1] = 0, \tag{7b}$$

where V_{g1} and V_{g2} are the (complex) group velocity of the envelopes F_1 and F_2, respectively. The second-order solution reads

$$A_1^{(2)} = \sum_{n=1}^{2} B_{1,2}|F_n|^2 e^{-\bar{\alpha}_n z_2}, \tag{8a}$$

$$A_{2,3}^{(2)} = i\frac{1}{\kappa A_4^{*(0)}}\left(\frac{1}{c} - \frac{1}{V_{g1,g2}^*}\right)\frac{\partial F_{1,2}^*}{\partial t_1}e^{-i\theta_{1,2}^*}, \tag{8b}$$

$$A_4^{(2)} = -\frac{1}{d_4}\sum_{n=1}^{2}\left(\frac{K_{1,2}^* - \omega/c}{\kappa A_4^{*(0)}} + \Omega_P B_{1,2}\right)|F_{1,2}|^2 e^{-\bar{\alpha}_{1,2}z_2}, \tag{8c}$$

with

$$B_{1,2} = \frac{1}{2\kappa A_1^{(0)}(1+|\Omega_P/d_4|^2)} \times\left[\frac{K_{1,2} - \omega/c}{d_4^*} + \frac{K_{1,2}^* - \omega/c}{d_4} - \frac{|K_{1,2} - \omega/c|^2}{\kappa|A_4^{(0)}|^2}\right], \tag{9}$$

where $\alpha_1 = \varepsilon^2\bar{\alpha}_1$ ($\alpha_2 = \varepsilon^2\bar{\alpha}_2$).

At the third ($O(\varepsilon^3)$) order, divergence-free conditions yield the coupled nonlinear equations for F_1 and F_2:

$$i\frac{\partial F_1}{\partial z_2} - \frac{K_{21}}{2}\frac{\partial^2 F_1}{\partial t_1^2} - (W_{11}|F_1|^2 + W_{12}|F_2|^2)F_1 = 0, \quad (10a)$$

$$i\frac{\partial F_2}{\partial z_2} - \frac{K_{22}}{2}\frac{\partial^2 F_2}{\partial t_1^2} - (W_{21}|F_1|^2 + W_{22}|F_2|^2)F_2 = 0, \quad (10b)$$

where

$$W_{11,22} = \frac{\kappa|\Omega_P|^2}{d_{2,3}^*|d_{2,3}|^2}\frac{d_{2,3}d_4 + (d_{2,3}d_4)^* - |\Omega_P|^2}{(|d_4|^2 + |\Omega_P|^2)^2}, \quad (11a)$$

$$W_{12,21} = \frac{\kappa|\Omega_P|^2}{d_{2,3}^*|d_{3,2}|^2}\frac{d_{3,2}d_4 + (d_{3,2}d_4)^* - |\Omega_P|^2}{(|d_4|^2 + |\Omega_P|^2)^2}, \quad (11b)$$

are the coefficients of SPM (W_{11} and W_{22}) and CPM (W_{12} and W_{21}), respectively. It is easy to prove that these nonlinear coefficients satisfy the relation $W_{11}W_{22}=W_{12}W_{21}$, resulting from the symmetry of the configuration of the system.

4. WEAK-LIGHT SUPERLUMINAL VECTOR OPTICAL SOLITON SOLUTIONS

We now consider possible soliton solutions of the coupled nonlinear equations (10a) and (10b), which can be converted into the following dimensionless form:

$$i\left(\frac{\partial}{\partial s} + g_{A1}\right)u_1 + ig_\delta\frac{\partial u_1}{\partial \sigma} - g_{D1}\frac{\partial^2 u_1}{\partial \sigma^2} - 2(g_{11}|u_1|^2 + g_{12}|u_2|^2)u_1 = 0, \quad (12a)$$

$$i\left(\frac{\partial}{\partial s} + g_{A2}\right)u_2 - ig_\delta\frac{\partial u_2}{\partial \sigma} - g_{D2}\frac{\partial^2 u_2}{\partial \sigma^2} - 2(g_{22}|u_2|^2 + g_{21}|u_1|^2)u_2 = 0. \quad (12b)$$

Note that, while obtaining the above equations, we have introduced the dimensionless variables $s=z/(2L_D)$, $\sigma=(t-z/V_g)/\tau_0$, $u_1=(\Omega_{s1}/U_0)\exp[-i\,\mathrm{Re}(K_{01})z]$, and $u_2=(\Omega_{s2}/U_0)\exp[-i\,\mathrm{Re}(K_{02})z]$. The coefficients are defined by $g_{A1}=\alpha_1 L_D$, $g_{A2}=\alpha_2 L_D$, $g_\delta=2\,\mathrm{sign}(\delta)L_D/L_\delta$, $g_{D1}=K_{12}/|K_{22}|$, $g_{D2}=\mathrm{sign}(K_{22})$ and $g_{11,12,21,22}=W_{11,12,21,22}/|W_{22}|$, with $\delta=(1/V_{g1}-1/V_{g2})/2$ and $V_g=2V_{g1}V_{g2}/(V_{g1}+V_{g2})$. $L_D=\tau_0^2/|K_{22}|$ is characteristic dispersion length, $L_\delta=\tau_0/|\delta|$ is characteristic group velocity mismatch length, with τ_0 being characteristic pulse length of the signal field. Since our aim is to obtain solitonlike solutions, in Eqs. (12a) and (12b) we have assumed L_D is equal to the characteristic nonlinear length of the system, defined by $L_{NL}=1/(U_0^2|W_{22}|)$.

In general, Eqs. (12a) and (12b) are two coupled Ginzburg–Landau equations with complex coefficients. However, if a realistic parameter set can be chosen (see below) so that these coefficients become real, Eqs. (12a) and (12b) can be reduced into two coupled NLS equations and, hence, one can obtain shape-preserving soliton solutions. The coupled NLS equations admit bright–bright, bright–dark, and dark–dark vector soliton solutions through a balance between the dispersion and nonlinear effects [11]. The bright–bright vector soliton solution reads

$$u_{1,2} = \mathcal{V}_{1,2}\,\mathrm{sech}\,\sigma\exp[i(\mathcal{P}_{1,2}\sigma + \mathcal{Q}_{1,2}s)], \quad (13)$$

if the condition $g_{22}g_{D1}=g_{12}g_{D2}$ can be fulfilled. Here we have defined $\mathcal{P}_1=g_\delta/(2g_{D1})$, $\mathcal{P}_2=-g_\delta/(2g_{D2})$, $\mathcal{Q}_1=-g_\delta^2/(4g_{D1})-g_{D1}$ ($\mathcal{Q}_2=-g_\delta^2/(4g_{D2})-g_{D2}$), and $\mathcal{V}_2=[(g_{D1}-g_{11}\mathcal{V}_1^2)/g_{12}]^{1/2}$. A bright–dark vector soliton solution is given by

$$u_1 = \mathcal{V}_1\,\mathrm{sech}\,\sigma\exp[i(\mathcal{P}_1\sigma + \mathcal{Q}_1 s)], \quad (14a)$$

$$u_2 = \mathcal{V}_2\tanh\sigma\exp[i(\mathcal{P}_2\sigma + \mathcal{Q}_2 s)] \quad (14b)$$

under the same condition given above, where $\mathcal{P}_1=g_\delta/(2g_{D1})$, $\mathcal{P}_2=-g_\delta/(2g_{D2})$, $\mathcal{Q}_1=-\mathcal{P}_1 g_\delta - g_{D1}(1-\mathcal{P}_1^2)-2g_{12}\mathcal{V}_2^2$, $\mathcal{Q}_2=\mathcal{P}_2 g_\delta + g_{D2}\mathcal{P}_2^2 - 2g_{22}\mathcal{V}_2^2$, and $\mathcal{V}_2=[(g_{11}\mathcal{V}_1^2-g_{D1})/g_{12}]^{1/2}$. In both solutions given by Eqs. (13) and (14), $\mathcal{V}_1$ is a free real parameter.

To demonstrate that the imaginary parts of the coefficients of Eqs. (12a) and (12b) can be much less than their corresponding real parts, we consider a set of realistic parameters relevant to a ^{87}Rb alkali atom vapor [30]. The atomic levels can be chosen as $|1\rangle=|5S_{1/2},F=1,m_F=0\rangle$, $|2\rangle=|5S_{1/2},F=1,m_F=+1\rangle$, $|3\rangle=|5S_{1/2},F=1,m_F=-1\rangle$, and $|4\rangle=|5P_{1/2},F'=1,m_{F'}=0\rangle$. For such system working at temperature (around 300 K), the Doppler effect may contribute linewidth broadening around 500 MHz, which may degrade the effectiveness of an EIT-based scheme. It is, however, much less important in an ARG-based scheme, because we can choose a large one-photon detuning Δ_4 to suppress the Doppler effect. This can be easily reached by taking $\Delta_4=-2.0$ GHz in the present system. Specifically, the parameters are given by $2\gamma_2\approx 2\gamma_3=300$ Hz, $2\gamma_4=500$ MHz (a large value of γ_4 is mainly due to Doppler broadening), $\kappa=1.0\times10^{10}\ \mathrm{cm^{-1}\,s^{-1}}$, $\Omega_P=4.0\times10^7\ \mathrm{s^{-1}}$, $\Delta_2=3.1\times10^6\ \mathrm{s^{-1}}$, $\Delta_3=2.9\times10^6\ \mathrm{s^{-1}}$ (i.e., $\Delta=2.0\times10^5\ \mathrm{s^{-1}}$), $\lambda_p=c/\nu_p=0.8\times10^{-4}$ cm, and $\tau_0=0.7\times10^{-6}$ s. With these parameters we get $K_{01}=-(1.27+i0.06\times10^{-3})\mathrm{cm^{-1}}$, $K_{02}=-(1.36+i0.07\times10^{-3})\mathrm{cm^{-1}}$ (i.e., $\alpha_1=-0.12\times10^{-3}\ \mathrm{cm^{-1}}$, $\alpha_2=-0.14\times10^{-3}\ \mathrm{cm^{-1}}$), $K_{11}=-(40.96+i0.004)\times10^{-8}\ \mathrm{cm^{-1}\,s}$, $K_{12}=-(46.81+i0.005)\times10^{-8}\ \mathrm{cm^{-1}\,s}$, $K_{21}=-(26.43+i0.004)\times10^{-14}\ \mathrm{cm^{-1}\,s^2}$, $K_{22}=-(32.28+i0.005)\times10^{-14}\ \mathrm{cm^{-1}\,s^2}$, $W_{11}=-(45.52+i0.002)\times10^{-17}\ \mathrm{cm^{-1}\,s^2}$, $W_{12}=-(49.05+i0.002)\times10^{-17}\ \mathrm{cm^{-1}\,s^2}$, $W_{21}=-(48.66+i0.003)\times10^{-17}\ \mathrm{cm^{-1}\,s^2}$, and $W_{22}=-(52.43+i0.003)\times10^{-17}\ \mathrm{cm^{-1}\,s^2}$. We see that the imaginary part of the coefficients are indeed much smaller than their corresponding real part. With these results we obtain $L_D=L_{NL}=1.5$ cm and $L_\delta=24$ cm. The system works in an anomalous dispersion region with the group velocity given by

$$V_{g1} = -8.1\times10^{-5}c \quad (\text{for } \sigma_- \text{ component}), \quad (15)$$

$$V_{g2} = -7.1\times10^{-5}c \quad (\text{for } \sigma_+ \text{ component}), \quad (16)$$

respectively. Consequently, *the obtained vector optical soliton travels with superluminal propagating velocity*.

Shown in Fig. 2(a) is the result of numerical simulation on the evolution of σ^- component of the signal field versus

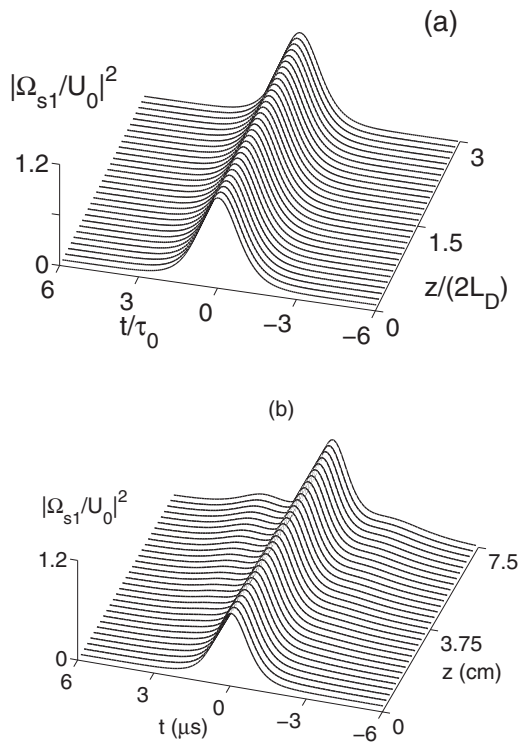

Fig. 2. (a) Waveshape of $|\Omega_{s1}/U_0|^2$ obtained by numerically integrating Eq. (12) with the bright-bright soliton solution as an initial condition. (b) Waveshape of $|\Omega_{s1}/U_0|^2$ obtained by numerically integrating Eqs. (3) and (5) with the same initial condition. (Waveshape of $|\Omega_{s2}/U_0|^2$ is similar to $|\Omega_{s1}/U_0|^2$ and hence not shown.) The parameters are given in the text [just below Eq. (14)].

dimensionless time t/τ_0 and distance $z/(2L_D)$ with the above parameters. (The evolution of σ^+ component is very similar thus not shown.) The simulation is made by numerically integrating Eqs. (12a) and (12b) and the bright–bright soliton solution (13) as an initial condition. We see that the superluminal vector optical soliton can propagate stably over a long distance.

In order to make further confirmation on the superluminal vector optical soliton solutions and check their stability, we have done additional numerical simulations starting directly from Eqs. (3) and (5) with the same parameters and initial condition. Shown in Fig. 2(b) is the waveshape of $|\Omega_{s1}/U_0|^2$ after propagating to $z=7.5$ cm. One can see that the pulse shape suffers no serious distortion except for some small radiations (ripples) appearing on its two wings due to the contribution of the high-order dispersion and high-order nonlinear effects that have not been included in the analytical approach given above. Thus the superluminal vector soliton in the system is indeed rather robust during propagation.

The input power of the vector optical soliton can be estimated by Poynting's vector. It is easy to get the average flux of energy over carrier-wave period $\bar{P}_1=\bar{P}_1^{\max}\,\mathrm{sech}^2[(t-z/V_{g1})/\tau_0]$ and $\bar{P}_2=\bar{P}_2^{\max}\,\mathrm{sech}^2[(t-z/V_{g2})/\tau_0]$, with the peak power

$$\bar{P}_1{}^{\max}\approx\bar{P}_2{}^{\max}=5.2\times10^{-3}\ \mathrm{mW}. \tag{17}$$

When obtaining this result we have taken $|\mathbf{p}_{23}|\approx|\mathbf{p}_{43}|=2.1\times10^{-27}$ cm C and the beam radius of the signal laser as $R_\perp=0.01$ cm. We see that, *to generate the superluminal optical vector soliton in this ARG system, only very low input power is needed*.

Notice that the weak-light vector solitons produced in the present ARG system have many obvious advantages over those based on EIT systems [18]. One of the advantages is that the ARG system can work at room temperature and the vector solitons in such system suffer no serious absorption or Doppler effect. Another one is that the vector solitons generated in the ARG scheme can travel with superluminal propagating velocity, which is very promising for the design of rapidly responding all-optical devices [30,31].

Since the parameters of the present ARG system can be actively manipulated, the coefficients of Eqs. (12a) and (12b) can be easily tuned to allow a Manakov system to be realized[36], which is a completely integrable and supports multisoliton solutions. In fact, with the parameters of the ^{87}Rb system given just below Eq. (14), we have $g_{A1}\simeq g_{A2}=-0.2\times10^{-3}$, $g_\delta=0.1$, $g_{D1}=-0.8$, $g_{D2}=-1.0$, $g_{11}\simeq g_{12}\simeq g_{21}=-0.9$, and $g_{22}=-1.0$. Then Eqs. (12a) and (12b) can be written into the perturbed Manakov equations

$$i\frac{\partial u_1}{\partial s}+\frac{\partial^2 u_1}{\partial\sigma^2}+2(|u_1|^2+|u_2|^2)u_1=R_1, \tag{18a}$$

$$i\frac{\partial u_2}{\partial s}+\frac{\partial^2 u_2}{\partial\sigma^2}+2(|u_2|^2+|u_1|^2)u_2=R_2, \tag{18b}$$

with R_1, R_2 being small quantities. When R_1 and R_2 are neglected, one obtains the bright vector soliton solution of Manakov equations [37–39]:

$$u_1=\frac{p_1e^{\eta_1}+p_2e^{\eta_2}+e^{\eta_1+\eta_1^*+\eta_2+d_1}+e^{\eta_1+\eta_2+\eta_2^*+d_2}}{1+e^{\eta_1+\eta_1^*+r_1}+e^{\eta_1+\eta_2^*+d_0}+e^{\eta_1^*+ta_2+d_0^*}+e^{\eta_2+\eta_2^*+r_2}+e^{\eta_1+\eta_1^*+\eta_2+\eta_2^*+r_3}}, \tag{19a}$$

$$u_2=\frac{q_1e^{\eta_1}+q_2e^{\eta_2}+e^{\eta_1+\eta_1^*+\eta_2+d_1'}+e^{\eta_1+\eta_2+\eta_2^*+d_2'}}{1+e^{\eta_1+\eta_1^*+r_1}+e^{\eta_1+\eta_2^*+d_0}+e^{\eta_1^*+ta_2+d_0^*}+e^{\eta_2+\eta_2^*+r_2}+e^{\eta_1+\eta_1^*+\eta_2+\eta_2^*+r_3}}, \tag{19b}$$

where

$$e^{d_0}=\frac{c_{12}}{w_1+w_2^*},\quad e^{r_1}=\frac{c_{11}}{w_1+w_1^*},\quad e^{r_2}=\frac{c_{22}}{w_2+w_2^*},$$

$$e^{d_1}=\frac{w_1-w_2}{(w_1+w_1^*)(w_1^*+w_2)}(p_1c_{21}-p_2c_{11}),$$

$$e^{d_2}=\frac{w_2-w_1}{(w_2+w_2^*)(w_1+w_2^*)}(p_2c_{12}-p_1c_{22}),$$

$$e^{d_1'}=\frac{w_1-w_2}{(w_1+w_1^*)(w_1^*+w_2)}(q_1c_{21}-q_2c_{11}),$$

$$e^{d_2'}=\frac{w_2-w_1}{(w_2+w_2^*)(w_1+w_2^*)}(q_2c_{12}-q_1c_{22}),$$

$$e^{r_3}=\frac{|w_1-w_2|^2}{(w_1+w_1^*)(w_2+w_2^*)|w_1+w_2^*|^2}(c_{11}c_{22}-c_{12}c_{21}),$$

with $c_{ij}=(p_ip_j^*+q_iq_j^*)/(w_i+w_j^*)$, $\eta_i=w_i(\sigma+iw_is)$, p_j, q_j, w_j ($j=1,2$) being arbitrary complex parameters.

Although the total energy of the vector soliton is conserved, the distribution of the energy density for each component may change due to the interaction between two components. In fact, both elastic and inelastic collisions can be obtained by changing the relative phase of p_i and q_i. In Fig. 3, we have plotted the intensity profiles in two different cases of σ^- component of the signal field versus dimensionless time t/τ_0 and distance $z/(2L_D)$. (The evolution of the σ^+ component is omitted here.) The system is still based on the ^{87}Rb atom, and the physical parameters are the same as those used in Fig. 2. In the simulation in Fig. 3(a), Eq. (19) is chosen as an initial condition with $w_1=1+i$, $w_2=1.5-i$, and $p_1=p_2=q_1=q_2=1$. The result is obtained by numerically integrating Eqs. (18a) and (18b), where small perturbations R_1 and R_2 have been taken into account. We see that, in this case, an elastic collision between two σ^- components of vector solitons is realized. In panel (c), the initial condition is still Eq. (19), but taking $p_2=e^{i\phi}$ with $\phi\asymp 64°$. One sees that, in this case, an inelastic collision occurs instead. In Figs. 3(b) and 3(d), we show the waveshape of $|\Omega_{s1}/U_0|^2$ after propagating to $z=7.5$ cm with the same initial conditions as those used in Figs. 3(a) and 3(c). The results are obtained by numerical simulations starting directly from Eqs. (3) and (5).

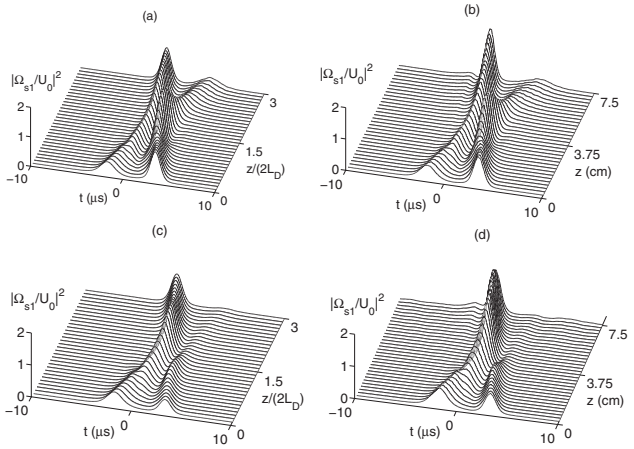

Fig. 3. The intensity profiles of collision between two σ^- components of superluminal vector solitons. (a) and (b): Waveshape of $|\Omega_{s1}/U_0|^2$ with $w_1=1+i$, $w_2=1.5-i$, and $p_1=p_2=q_1=q_2=1$. (c) and (d): Waveshapes of $|\Omega_{s1}/U_0|^2$ with $w_1=1+i$, $w_2=1.5-i$, $p_1=q_1=q_2=1$, and $p_2=e^{i\phi}$ ($\phi\asymp 64°$). The results in (a) and (c) are obtained by numerically integrating Eqs. (18a) and (18b), where small perturbations R_1 and R_2 have been taken into account. The results in (b) and (d) are obtained by numerically integrating Eqs. (3) and (5). The parameters are the same as those used in Fig. 2.

The results obtained here raise the possibility of realizing new types of optical soliton switching and logic gates. Because group velocities of the two components of superluminal vector optical solitons are well matched and faster than light speed in vacuum, the switching and logic gates based on such superluminal vector optical solitons can be very fast [30,31].

5. DISCUSSION AND SUMMARY

We have proposed a scheme to generate and propagate superluminal vector optical solitons based on a room-temperature four-level ARG medium. Contrary to the previously used EIT-based scheme, which is absorptive in nature, the new scheme is based on the key idea of the signal field operating in a stimulated Raman emission mode and, hence, can eliminate all attenuation and distortion at room temperature. By means of a method of multiple scales we have derived a couple of NLS equations that govern the envelope evolution of two polarization components of the signal field. Superluminal Manakov vector soliton solutions have been obtained under a set of realistic physical parameters associated with ^{87}Rb atoms. We have shown that the input power needed for generating superluminal vector optical solitons can be very low. We have carried out a numerical simulation for checking the stability of the superluminal vector optical solitons and demonstrated that such vector solitons are rather robust. We have also made a numerical investigation on the collision between two bright superluminal vector optical solitons. Both elastic and inelastic collisions have been observed, thereby raising the possibility of designing rapidly responding optical switching and logic gates based on the superluminal vector optical solitons in the ARG system working at room temperature.

ACKNOWLEDGMENTS

The authors thank L. Deng for useful discussions. This work was supported by the National Natural Science Foundation of China (NSFC) under grants 10674060 and 10874043, by the Key Development Program for Basic Research of China under grants 2005CB724508 and 2006CB921104, and by the Program for Changjiang Scholars and the Innovative Research Team of the Chinese Ministry of Education.

REFERENCES

1. C. R. Menyuk, "Stability of solitons in birefringent optical fibers. I: Equal propagation amplitudes," Opt. Lett. **12**, 614–616 (1987).
2. D. N. Christodoulides and R. I. Joseph, "Vector solitons in birefringent nonlinear dispersive media," Opt. Lett. **13**, 53–55 (1988).
3. M. V. Tratnik and J. E. Sipe, "Bound solitary waves in a birefringent optical fiber," Phys. Rev. A **38**, 2011–2017 (1988).
4. Y. Barad and Y. Silberberg, "Polarization evolution and polarization instability of solitons in a birefringent optical fiber," Phys. Rev. Lett. **78**, 3290–3293 (1997).
5. A. E. Korolev, V. N. Nazarov, D. A. Nolan, and C. M. Truesdale, "Experimental observation of orthogonally polarized time-delayed optical soliton trapping in birefringent fibers," Opt. Lett. **30**, 132–134 (2005).
6. D. Rand, I. Glesk, C. -S. Brès, D. A. Nolan, X. Chen, J. Koh, J. W. Fleischer, K. Steiglitz, and P. R. Prucnal, "Observation of temporal vector soliton propagation and collision in birefringent fiber," Phys. Rev. Lett. **98**, 053902 (2007).
7. M. Segev, G. C. Valley, B. Crosignani, P. DiPorto, and A. Yariv, "Steady-state spatial screening solitons in photorefractive materials with external applied field," Phys. Rev. Lett. **73**, 3211–3214 (1994).
8. J. U. Kang, G. I. Stegeman, J. S. Aitchison, and N. Akhmediev, "Observation of Manakov spatial solitons in AlGaAs planar waveguides," Phys. Rev. Lett. **76**, 3699–3702 (1996).
9. M. Delquè, T. Sylvestre, H. Maillotte, C. Cambournac, P. Kockaert, and M. Haelterman, "Experimental observation of the elliptically polarized fundamental vector soliton of isotropic Kerr media," Opt. Lett. **30**, 3383–3385 (2005).
10. M. N. Islam, *Ultrafast Fiber Switching Devices and Systems* (Cambridge U. Press, 1992).
11. G. P. Agrawal, *Nonlinear Fiber Optics* (Elsevier (Singapore), 2004).
12. S. T. Cundiff, B. C. Collings, N. N. Akhmediev, J. M. Soto-Crespo, K. Bergman, and W. H. Knox, "Observation of polarization-locked vector solitons in an optical fiber," Phys. Rev. Lett. **82**, 3988–3991 (1999).
13. M. Fleischhauer, A. Imamoglu, and J. P. Marangos, "Electromagnetically induced transparency: Optics in coherent media," Rev. Mod. Phys. **77**, 633–673 (2005), and references therein.
14. Y. Wu and L. Deng, "Ultraslow optical solitons in a cold four-state medium," Phys. Rev. Lett. **93**, 143904 (2004).
15. G. Huang, L. Deng, and M. G. Payne, "Dynamics of ultraslow optical solitons in a cold three-state atomic system," Phys. Rev. E **72**, 016617 (2005).
16. L. Deng, M. G. Payne, G. Huang, and E. W. Hagley, "Formation and propagation of matched and coupled ultraslow optical soliton pairs in a four-level double-system," Phys. Rev. E **72**, 055601(R) (2005).
17. C. Hang, G. Huang, and L. Deng, "Generalized nonlinear Schrödinger equation and ultraslow optical solitons in a cold four-state atomic system," Phys. Rev. E **73**, 036607 (2006).
18. C. Hang and G. Huang, "Weak-light ultraslow vector solitons via electromagnetically induced transparency," Phys. Rev. A **77**, 033830 (2008).
19. R. W. Boyd and D. J. Gauthier, *Progress in Optics* (Elsevier Science, 2002), Vol. 43, Chap. 6, p. 275 and references therein.
20. S. Chu and S. Wong, "Linear pulse propagation in an absorbing medium," Phys. Rev. Lett. **48**, 738–741 (1982).
21. R. Y. Chiao, "Superluminal (but causal) propagation of wave packets in transparent media with inverted atomic populations," Phys. Rev. A **48**, R34–R37 (1993).
22. A. M. Steinberg and R. Y. Chiao, "Dispersionless, highly superluminal propagation in a medium with a gain doublet," Phys. Rev. A **49**, 2071–2075 (1994).
23. L. J. Wang, A. Kuzmich, and P. Pogariu, "Superluminal solitons in a Λ-type atomic system with two-folded levels," Nature (London) **406**, 277–279 (2000).
24. A. Dogariu, A. Kuzmich, and L. J. Wang, "Transparent anomalous dispersion and superluminal light-pulse propagation at a negative group velocity," Phys. Rev. A **63**, 053806 (2001).
25. M. D. Stenner, D. J. Gauthier, and M. A. Neifeld, "The speed of information in a fast-light optical medium," Nature (London) **425**, 695–698 (2003).
26. M. D. Stenner and D. J. Gauthier, "Pump-beam-instability limits to Raman-gain-doublet fast-light pulse propagation," Phys. Rev. A **67**, 063801 (2003).
27. L.-G. Wang, N.-H. Liu, Q. Lin, and S.-Y. Zhu, "Superluminal propagation of light pulses: A result of interference," Phys. Rev. E **68**, 066606 (2003).
28. H. Kang, G. Hernandez, and Y. Zhu, "Superluminal and slow light propagation in cold atoms," Phys. Rev. A **70**, 011801 (2004).
29. K. J. Jiang, L. Deng, and M. G. Payne, "Ultraslow propagation of an optical pulse in a three-state active Raman gain medium," Phys. Rev. A **74**, 041803(R) (2006).
30. L. Deng and M. G. Payne, "Gain-assisted large and rapidly responding Kerr effect using a room-temperature active Raman gain medium," Phys. Rev. Lett. **98**, 253902 (2007).
31. K. J. Jiang, L. Deng, E. W. Hagley, and M. G. Payne, "Fast-responding nonlinear phase shifter using a signal-wave gain medium," Phys. Rev. A **77**, 045804 (2008).
32. B. D. Clader and J. H. Eberly, "Theoretical study of fast light with short sech pulses in coherent gain media," J. Opt. Soc. Am. B **24**, 916–921 (2007).
33. G. S. Agarwal and T. N. Dey, "Fast light solitons in resonant media," Phys. Rev. A **75**, 043806 (2007).
34. G. Huang, C. Hang, and L. Deng, "Gain-assisted superluminal optical solitons at very low light intensity," Phys. Rev. A **77**, 011803(R) (2008).
35. H. Li, C. Hang, and G. Huang, "High-order nonlinear Schrödinger equation and superluminal optical solitons in room-temperature active-Raman-gain media," Phys. Rev. A **78**, 023822 (2008).
36. S. V. Manakov, "On the theory of two-dimensional stationary self-focusing of electromagnetic waves," Sov. Phys. JETP **38**, 248–253 (1974).
37. R. Radhakrishnan, M. Lakshmanan, and J. Hietarinta, "Inelastic collision and switching of coupled bright solitons in optical fibers," Phys. Rev. E **56**, 2213–2216 (1997).
38. T. Kanna and M. Lakshmanan, "Exact soliton solutions, shape changing collisions, and partially coherent solitons in coupled nonlinear Schrödinger equations," Phys. Rev. Lett. **86**, 5043 (2001).
39. T. Kanna and M. Lakshmanan, "Exact soliton solutions of coupled nonlinear Schrödinger equations: Shape-changing collisions, logic gates, and partially coherent solitons," Phys. Rev. E **67**, 046617 (2003).